Molecular dynamics in polymer networks containing caprolactone and ethylene glycol moieties studied by dielectric relaxation spectroscopy

R. Sabater i Serra[1*], J.L. Escobar Ivirico[1], F. Romero Colomer[1], A. Andrio Balado[2], J.L. Gómez Ribelles[1,3]

[1]Center for Biomaterials and Tissue Engineering. Universitat Politècnica de València, 46022 València, Spain

[2]Departament de Física, Universitat Jaume I, 12071 Castelló, Spain

[3]CIBER en Bioingeniería, Biomateriales y Nanomedicina, Valencia, Spain

[*] **Corresponding author:** Roser Sabater i Serra

e-mail: rsabater@die.upv.es

Keywords: copolymer networks, hydrogels, dielectric relaxation, molecular mobility

Abstract

Copolymer networks with methacrylate main chain and caprolactone and ethylene glycol side groups were obtained by free radical copolymerization of caprolactone methacrylate (CLMA) and poly(ethylene glycol) methacrylate (PEGMA). Dielectric relaxation spectroscopy was used to analyse molecular mobility of the different groups in the system. Only one main dielectric relaxation process was found in CLMA/PEGMA copolymer networks, located between those of the corresponding homonetworks, indicating that the system does not present phase separation. The copolymers show a secondary relaxation process at temperatures below -50ºC, which can be assigned to the overlapping of the corresponding secondary processes for the homopolymer networks; one of them related to the local mobility of caprolactone units in CLMA and the second one assigned to the twisting motions within ethylene glycol moiety in PEGMA. Besides the relaxation processes, the mobility of space charges has been analysed by means of conductivity and electric modulus formalisms.

1. Introduction

Poly(ethylene glycol), PEG, hydrogels have been frequently used to encapsulate and culture different types of cells in three dimensional environments for tissue engineering applications. It has been shown that elastic properties and cross-linking density of these gels influence in large extent the biological response [1, 2]. It is well known that PEG is not adhesive for cells, as probed in monolayer culture of a variety of cells [3]. On the other hand it has been shown very good attachment of different cells to poly (caprolactone methacrylate) substrates both in monolayer and in 3D supports.

Recently our group presented polymer networks that combine these two materials in order to modulate cell adhesion response for neural regeneration [4]. The polymer network was produced by copolymerization of caprolactone methacrylate, CLMA, and poly(ethylene gycol) methacrylate, PEGMA. The result of the polymerization is a methacrylate main chain with side chains containing caprolactone and/or poly(ethelene glycol) groups. These networks absorb increasing amounts of water with increasing PEGMA contents [4] while caprolactone segments provide attachement points for proteins that mediate cell adhesion.

We hypothesise that the behaviour of these materials as cell culture supports is in large extent determined by the spatial distribution and mobility of the different molecular groups. The main objective of this work is to provide a deeper insight in the structure of the system by means of dielectric relaxation spectroscopy (DRS), analyzing the relaxational modes that take place in the networks as a function of the CLMA/PEGMA ratio in the copolymers. Dielectric relaxation spectroscopy (DRS) is a powerful technique in investigating molecular mobility in polymer systems with the advantage that it can be used in an extremely wide frequency range analysis, from mHz to GHz [5]. This technique, together with dynamic-mechanical spectroscopy and differential scanning calorimetry has been extensively used to study the structure and molecular mobility of polymers, polymer blends [6-10] and copolymers [11-13].

2. Materials and methods

2.1 Materials

Caprolactone 2-(methacryloyloxy)ethyl ester (CLMA), purchased from Sigma-Aldrich with a molecular weight of 244.28 g/mol and poly (ethylene glycol) methacrylate (PEGMA) (Sigma-Aldrich, 96% pure) with a molecular weight of 526 g(mol were employed without further purification. Ethylene glycol dimethacrylate (EGDMA) (Aldrich, 99% pure) and 2,2'Azobisisobutyronitrile (AIBN) (Aldrich, 98% pure) were used as crosslinking agent and initiator respectively. As solvent N,N-Dimethylformamide (DMF) (Aldrich, 99.8% pure) and ethanol (Aldrich, 99.5% pure) were employed.

2.2 Preparation of the samples

Copolymer networks were synthesised by radical polymerization. Different proportions of CLMA and PEGMA (30/70, 50/50 and 70/30) were dissolved in DMF (50 wt%). 0.1 wt% of AIBN and 1 wt% of EGDMA were employed as initiator and crosslinker respectively. The reaction was carried out at 60 ºC for 24 h. Low molecular weight substances were extracted by boiling in ethanol for 24 h and dried in vacuum until constant weight. The homopolymer networks were obtained applying the same procedure. The molecular structures of both monomers and copolymer are shown in the schemas of Figure 1.

The samples obtained were designed as polyCLMA and polyPEGMA for the homopolymers networks and poly(CLMA-co-PEGMA) XX/YY for copolymer networks, where XX and YY are the weight ratio of CLMA and PEGMA respectively, The molecular weight obtained for the copolymers 30/70, 50/50 and 70/30 was 291.04, 333.62 and 390.79 g/mol respectively [4].

2.3. Experiments

The measurements were carried out in an impedance analyser ALPHA-S (Novocontrol Technologies) in a frequency range from 0.1 Hz to 1 MHz. Samples around 0.5 mm thickness were dried in vacuum at 25 ºC for 48h to remove traces of humidity. After that, the samples were placed in a parallel plate capacitor with 10 mm of diameter mounted on a temperature controlled cryostat (BDS 1100) and exposed to a heated gas stream evaporated from a liquid nitrogen Deward. The temperature control was assured

by a Quatro Cryosystem from Novocontrol GMbH. The isothermal experiments were performed from -140 ºC up to 100 ºC with a thermal stability of 0.5 ºC and the complex permittivity, $\varepsilon^*=\varepsilon'+i\varepsilon''$, were determined as a function of frequency each 5 ºC. The standard deviation in the measurements motivated by the uncertainties in the determination of the sample thickness is lower than 6%.

3. Results

Figure 2 shows the dielectric loss factor (ε'') for polyCLMA network in the interval from -130 ºC to 50 ºC. Two dipolar relaxation processes can be identified, a low temperature process, shown between -140 ºC and -50 ºC (Figure 2a), and at higher temperatures, between 20 ºC and 90 ºC (Figure 2b), a second one overlapped with conductivity.

The temperature dependence of the dielectric loss factor for both homopolymers and copolymers networks is shown in Figure 3 at $1\cdot10^4$ Hz. The homopolymer networks polyCLMA and polyPEGMA show a relaxation process between -120 ºC and -60 ºC, with lower amplitude for polyPEGMA network. Copolymer networks show a relaxation process in the same temperature interval, whose amplitude is between the corresponding homonetworks. This process has been analysed in the interval between -130 ºC and -85 ºC using the Havriliak-Negami function (HN) function [14]:

$$\varepsilon^* = \varepsilon' + i\varepsilon'' = \varepsilon_\infty + \sum_{k=1}^{n} \frac{\Delta\varepsilon_k}{\left[1+\left(i\omega\tau_k\right)^{a_k}\right]^{b_k}} \qquad (1)$$

where ε_∞ is the limit to high frequencies of the real component of the complex permittivity and the second term is the sum of the *n* independent relaxation processes. $\Delta\varepsilon$ is the relaxation strength, τ is the characteristic relaxation time and *a* and *b* are shape parameters ($0 < a \leq 1$, $0 < a\cdot b \leq 1$). The parameter *a* can be related to the width of the relaxation in the frequency domain while *b* accounts for its asymmetry. The fitting parameters are reported in Table 1.

At higher temperature, between -30 ºC and 60 ºC, a second relaxation process can be seen in all samples. In the homopolymers, the high temperature peak is located around -30ºC in polyPEGMA and around 60 ºC in polyCLMA; in the copolymers the peak is

placed between the homopolymer networks process. Above -5 ºC the dielectric loss factor, ε'', increases quickly and overlaps the high temperature relaxation process in samples with PEGMA content. This behaviour, related mainly to ohmic conductivity, is clearly shown in poly(CLMA-co-PEGMA) 50/50 and 70/30, where the maximum of the peak can not be identified.

The isothermal curves obtained at 70 ºC are shown in Figure 4 for all the samples. The relaxation process located al high temperature is distinctly defined for polyCLMA network, however, in the remaining samples the ohmic conduction overlaps with this relaxation process and it is no possible to identify the process. In order to minimise the presence of ohmic conduction, the dielectric loss factor ε'' has been obtained applying the derivative method [15]:

$$\varepsilon''_{der} \approx -\left(\frac{\pi}{2}\right)\frac{\partial \varepsilon'(\omega)}{\partial \ln \omega} \tag{2}$$

The inset of Figure 4 shows the curves obtained after applying the derivative method, where the high temperature relaxation is now clearly identified in all samples. At 70 ºC, the process is located between 1 kHz and 1 MHz. The maximum of the peak appears in polyCLMA and polyPEGMA around 20 kHz and 160 kHz respectively. The copolymers show the peak between those homopolymer networks, shifting to higher frequency with increasing the amount of PEGMA. This high temperature relaxation process is shown in Figure 5 for poly(CLMA-co-PEGMA) 70/30 after applying the derivative method (equation 2). In the plot, between 20 ºC and 80 ºC, the process appears at frequencies above 10 Hz. The inset of Figure 5 shows the real part of the complex permittivity, ε' at 50 ºC, where different processes can be identified. These processes will be further discussed in the next section.

Considering the important contribution of ohmic conduction in the dielectric response, the complex conductivity, σ^*, has been obtained from the complex permittivity results as:

$$\sigma^*(\omega) = \sigma' + i\sigma'' = \varepsilon_0 \omega \varepsilon''(\omega) + i\varepsilon_0 \omega \varepsilon'(\omega) \tag{3}$$

where ε_0 is the permittivity of free space.

The real part of the conductivity, σ', between 20 ºC and 90 ºC has been plotted in Figure 6 for poly(CLMA 100) (Figure 6a) and the copolymer with ratio 50/50 (Figure 6b). The

imaginary part of the conductivity, σ'' obtained at 90 ºC has been included in the insets. Both the real and the imaginary part of the conductivity increase significantly as PEGMA units are introduced in the system.

In addition, the complex electric modulus formalism M^* has been applied to analyse the conductivity behaviour. Using this formalism, the influence of permittivity and conductivity at low frequencies is minimised, emphasizing the small features at high frequencies, and the effects of the electrode polarization are suppressed [5, 16]. The complex electric modulus has been obtained from the complex permittivity as:

$$M^* = M' + iM'' = \frac{1}{\varepsilon^*} = \frac{\varepsilon'}{\varepsilon'^2 + \varepsilon''^2} + j\frac{\varepsilon''}{\varepsilon'^2 + \varepsilon''^2} \quad (4)$$

Figure 7 shows the imaginary part of the electric modulus (M''), the real part of the permittivity (ε'), and the imaginary part of the complex permittivity (ε'' from the measurements and ε''_{der} from equation 2) for polyCLMA (Figure 7a) and the copolymer 50/50 (Figure 7b) at 80 ºC. The peak related to the conductivity process can be seen in M'', located in the temperature interval where ε' remains almost constant and ε'' rises swiftly.

The electric field relaxation due to motions of charge carriers has been well described by the Davidson-Cole function [17]:

$$M^* = M_\infty \left(1 - \frac{1}{(1 + i\omega\tau)^\beta} \right) \quad (5)$$

where τ is the conductivity relaxation at the frequency where M'' reachs the maximum, M_∞ is the electric modulus at higher frequency and the shape parameter β describes the distribution of the relaxation times. The smaller the value of β, the larger the deviation from the Debye-type relaxation (β=1).

The relaxation times obtained from the conductivity process (M*) applying the Davidson-Cole function and the ones calculated from the dipolar relaxation processes have been represented in the Arrhenius plot shown in Figure 8. The glass transition temperature T_g from DSC results at 10 ºC/min [4] has been also included, considering 100 s as the relaxation time at T_g [18]. All processes shown in the Arrhenius plot will be discussed in further detail below.

4. Discussion

PolyCLMA network shows two dipolar relaxation processes. At low temperatures, between -130 ºC and -50 ºC (Figure 2a), a secondary relaxation process, γ_{CLMA}-relaxation, which is related to local mobility of caprolactone units [6, 13, 19-20]. At higher temperatures, above 20ºC, the main relaxation, α_{CLMA}-relaxation, associated with the glass transition, can be seen at frequencies above 100 Hz (Figure 2b and 4). This main process is also shown in the isochronal curves plotted in Figure 3 (around 60 ºC at 10^4 Hz). At low frequencies and between 20 ºC and 90 ºC, the isothermals curves show a fast rise in ε'' with increasing temperature (Figure 2b). Analysing ε' in this interval, two processes can be identified: electrode polarization and ohmic conductivity. In the inset of Figure 2b, the real and the imaginary part of the permittivity (in logarithmic scale) have been plotted at 60 ºC. At frequencies lower than 1 Hz, both ε' and ε'' increase with decreasing frequencies, characteristic behaviour of electrode polarization phenomenon. Between 1 Hz and 100 Hz, ε'' remains practically constant, indicating the presence of ohmic conductivity. At frequencies above 10^3, the spectrum shows the main relaxation process with a peak in ε'' and a step-like decrease in ε'.

PolyPEGMA spectrum shows a secondary dipolar relaxation, γ_{PEGMA}-relaxation, located in the same temperature interval that the secondary process γ_{CLMA}-relaxation in polyCLMA (Figure 3). This process is assigned to the twisting motions within ethylene glycol moiety [21-24]. At higher temperature, above the glass transition, the main relaxation process, α_{PEGMA}-relaxation is identified. In the isothermal curves, the process overlaps with conductivity and it is not possible its visualization (Figure 4). Nevertheless, after applying the derivative method (equation 2), the process is now clearly identified in a wide temperature range.

CLMA/PEGMA copolymers show behaviour between both homopolymers (Figure 3). The low temperature relaxation process, refered to as $\gamma_{CLMA/PEGMA}$-relaxation, is placed in the same interval that the secondary processes in both homopolymers, γ_{CLMA}-relaxation and γ_{PEGMA}-relaxation, and its amplitude is between those of the corresponding homonetworks, which could indicate an overlap of both processes. As the temperature interval for this process are located in the same temperature interval and the amplitude of the relaxation peak is between both homopolymers, we have analysed this process using only one term in Havriliak-Negami function (equation 1). In this way, we focus the study in the evolution of the parameters between both homopolymers.

Figure 8 shows the relaxation times, $\tau_{HN,}$ and the shape parameters, along with the dielectric strength are listed in Table 1. The dielectric strength, $\Delta\varepsilon$, is 1.78±0.10 and 0.92±0.05 for polyCLMA and polyEGMA respectively. In the copolymers, the dielectric strength is 1.51±0.20 for poly(CLMA-co-PEGMA) 70/30, 1.25±0.10 for the copolymer 50/50 and 1.09±0.10 for the composition 30/70. As the amount of PEGMA increases, the dielectric strength decreases according to the copolymer proportion. The same behaviour was found for the shape parameters, where both the width and symmetry of the peak in the copolymers show the same trend.

The temperature dependence of the relaxation times in this local process shows the characteristic Arrhenius behaviour:

$$\tau(T) = Ae^{\frac{E_a}{k_B T}} \tag{6}$$

where E_a is the activation energy, k_B is the Boltzmann constant and A the preexponential factor. Table 1 collects the data obtained from this process. The activation energy in polyCLMA is around 41 kJmol^{-1} (near the result obtained in [19] for the γ_{PCL}-relaxation]. For polyPEGMA, the activation energy, ca 38 kJmol^{-1}, is close to the TrEGDMA, DEGDMA and TeEGDMa either unreacted of after polymerization [21-25]. For the copolymers, the results vary between those obtained in the homonetworks. The results obtained, dielectric strength, shape parameters and activation energy, corroborate the assumption that this relaxation is the superposition of the secondary processes γ_{CLMA} and γ_{PEGMA} relaxations.

Only one dipolar relaxation is shown in the copolymers at high temperature, (Figure 3 and 4) in the interval where the main relaxation process takes place in polyCLMA and polyPEGMA. The fact that only one relaxation appears in this temperature range indicates the system does not present phase separation. This behaviour agrees with the DSC results [4], where the copolymers show only one glass transition process. In the isochronal curves plotted in Figure 3, the maximum of the peak related to this main relaxation is visible in poly(CLMA-co-PEGMA) 30/70, while in samples with 50 and 70% of PEGMA, the increase of the conductivity hides the maximum of the peak. After applying the derivative method (equation 2), this process is now distinctly identified, as further illustrated in the isothermal curves shown in the inset of Figure 4. The frequency where the peak shows a maximum is placed between those of the corresponding homonetworks. Figure 5 shows the dielectric response obtained from poly(CLMA-co-

PEGMA) 70/30 between 20 ºC and 10 ºC. The main relaxation is located at frequencies above 10 Hz, and at lower frequencies, a strong rise in the dielectric loss factor appears (inset in Figure 4). This phenomenon, associated with electrode polarization, occurs mainly for moderately to highly conducting samples and influences the dielectric properties at low frequencies [5]. When frequency increases, ε' becomes almost constant, which indicates ohmic conduction (between 10 and 100 Hz at 50 ºC) and at higher frequencies the main relaxation process is shown both in the real and the imaginary part of the dielectric response. All copolymers show a similar behaviour, increasing conductivity and electrode polarization when the content of PEGMA does.

In order to characterise the main relaxation process, the relaxation times were obtained from the frequency of the peak (f_{max}) in the isothermal curves after applying the derivative method (equation 2) and they are plotted in Figure 8. The process presents an enhanced departure from Arrhenius behaviour, showing the characteristic curvature of fragile glass formers. The curves were fitted by Vogel-Fulcher-Tamman (VFT) equation [26-28]:

$$\tau(T) = \tau_0 e^{\frac{B}{T-T_0}} \tag{7}$$

where τ_0 is the relaxation time for a infinite temperature and B is a constant. T_0 (Vogel temperature) is the temperature where all the chain motions in equilibrium are frozen, which is found 30-70 K below T_g. The fitting results are plotted in Figure 8 while the parameters are listed in Table 2. The Vogel temperature for the polyCLMA is ca 230 K and for polyPEGMA is around 185 K; the copolymers show values between both limit values, increasing its value as CLMA units do.

We have estimated the dielectric glass transition temperature, $T_{g\text{-diel}}$, replacing τ by 100 s in equation 7. since it is usual to characterise the entry in the glassy state by a relaxation time of this order [29]. $T_{g\text{-diel}}$ obtained is ca 272 K for CLMA 100, and ca 227 K for polyPEGMA (Table 2). In the copolymers, the $T_{g\text{-diel}}$ decreases when PEGMA units are introduced, following the same trend as the glass transition obtained from DSC results [4]. The glass transition temperature has been also plotted in Figure 8, showing that both results, DRS and calorimetric, are in good agreement.

If we replace the VFT expression (equation 7) in the activation energy equation,

$$E_a = R\frac{\partial \ln \tau}{\partial(1/T)} \tag{8}$$

it is possible to obtain the activation energy as a function of temperature:

$$E_a(T) = \frac{RB}{(1-T_0/T)^2} \tag{9}$$

The activation energy obtained for the main relaxation process at $T_{g\text{-diel}}$ (equation 9) changes from ca 365 kJmol^{-1} for polyCLMA until ca 195 kJmol^{-1} for polyPEGMA. The copolymers show values between the homonetworks (Table 2), showing an homogenous behaviour according to its composition.

Besides the relaxations of dipolar origin found in the range and below the glass transition temperature, the mobility of the space charges at higher temperature contributes to the dielectric response. In Figures 3, 4 and 7, the conductivity overlaps with the dipolar relaxation phenomena and it is strongly affected by the increase of PEGMA units in the system.

Figure 6 shows two different regimens for the conductivity process: at low frequencies the plateau is related to d.c. conductivity, with no frequency dependence, and for higher frequencies the dependence with temperature is an evidence of the so-solled a.c. conductivity. Increasing PEGMA content, the conductivity rises significantly and the change between d.c. and a.c. conductivity shifts to higher frequencies. This behavioural change is produced at 10^3 Hz in polyCLMA, in copolymer 50/50 is around $2.5\cdot10^4$ Hz and in polyPEGMA (not shown) the value increases until $1.58\cdot10^5$ Hz. At low frequencies an enhancement of the value in the imaginary part of the conductivity is shown, more noticeable when PEGMA content increases (see the arrows in Figure. 6). This effect, related to electrode polarization, is significantly affected by the presence of PEGMA in the samples. For polyCLMA the phenomenon is negligible, nevertheless it is noticeable in poly(PEGMA) and copolymers, Figure 6b shows the phenomenon, shown between 0.1 and 10 Hz, for poly(CLMA-co-PEGMA) 50/50.

For further analysis of the conductivity process, we have applied the transformation between complex permittivity into complex electric modulus M^* (equation 4). The characteristic peak related with conductivity in M'' spectrum (see Figure 7 for

polyCLMA and copolymer 50/50) has been studied by means of the Davidson-Cole function (equation 5). The β parameter values (Table 3), below one, implies a non-Debye relaxation process. PolyCLMA shows the lowest deviation from the Debye process (β=0.86), however the value decreases with increasing the amount of PEGMA until β=0.8 for polyPEGMA. The relaxation times obtained in the Davidson-Cole fitting, following Arrhenius behaviour, are plotted in Figure 8 (τ_{DC}). Applying the Arrhenius function (equation 6), the values calculated for both preexponential factor and activation energy (Table 3) show how the presence of PEGMA in the system produces a drop in the activation energy from ca 80 $kJmol^{-1}$ for polyCLMA network to around 70 $kJmol^{-1}$ when 30% of PEGMA is introduced. The conductivity in the samples with PEGMA may also be increased by the presence of small traces of water in the samples. Even if the samples were dried before any measurement, the hydrophilic nature of PEGMA may allow the absorption of water molecules during the measurements. As we have applied different functions to analyse the conductivity process, Figure 9 shows the relaxation times obtained from the maximum of the peak in M" (τ_M), τ_{DC} calculated from the Davidson-Cole function (the Arrhenius fitting has been also included) and the ones obtained from the critical value, τ_c, in σ' at the end of the plateau where the change between d.c and a.c. conductivity appears. The results show a good agreement, with no significant differences between them.

After the application of the derivative method (equation 2), a loss peak at frequencies below the primary structural relaxation can be seen (grey symbols in Figure 7). This peak is shown in all samples; however it is distinctly significant in samples with higher CLMA content. In the frequency interval where the peak appears, the loss factor is mainly dominated by conductivity (ε' remains constant and ε'' rises sharply). The peak obtained from the electric modulus (M'') has been also included in the figure and it is located very close to the one we are discussing. The presence of this peak can also be seen in the isothermal curve plotted in Figure 5 (grey symbols) for poly(CLMA-co-PEGMA) 70/30. The origin of this Debye-type process could be originated by interfacial polarization effects related to the sample preparation; that may lead to trap some small pores or gas bubbles within the sample [30]. The samples were prepared from dissolution; the presence of pores inside the network is a likely scenario that may explain the presence of his peak in the spectra.

5. Conclusions

The polymerization of caprolactone methacrylate (CLMA) and poly(ethylene glycol) methacrylate (PEGMA) networks results in random copolymer networks formed by methacrylate main chains with side chains containing caprolactone and/or poly(ethylene glycol) groups. CLMA homonetwork shows the main relaxation process above 0 ºC and a secondary process related to local mobility of caprolactone units around -50 ºC. PEGMA homonetwork shows the main process at lower temperature and a secondary process assigned to the twisting motions within ethylene glycol moiety located in the same temperature interval that the secondary relaxation shown by polyCLMA. Dielectric response in CLMA-co-PEGMA copolymers presents homogeneous behaviour between both homopolymers according to the copolymer proportion, with no phase separation. Only one main dielectric relaxation process was found, placed between those of the corresponding homonetworks, along with a secondary process which can be assigned to the overlapping of the secondary processes from the homopolymer networks. The mobility of space charges is strongly affected by the addition of PEGMA units in the system. The activation energy of the conductivity process, obtained by means of electric modulus formalism, diminishes significantly when increasing PEGMA content.

Acknowledgments

The support from the Spanish Ministry of Economy and Competitiveness (MINECO) and FEDER funds under the project MAT2012-38359-C03-01 is gratefully acknowledged.

References

[1] S.J. Bryant, T.T. Chowdhury, D.A. Lee, D.L. Bader, K.S.Anseth, Ann. Biomed. Eng. 32-3 (2004) 407-417.

[2] G.D. Nicodemus, S.J. Bryant, J. Biomech. 41-7 (2008) 1528-1536.

[3] J.A. Neff, P.A. Tresco, K.D. Caldwell, Biomaterials 20 (1999) 2377-2393.

[4] J.L. Escobar Ivirico, D.M. García Cruz, M.C. Aranque Monrós, C. Martínez-Ramos, M. Monleón Pradas, J Mater Sci: Mater Med 23 (2012) 1605-1617.

[5] F. Kremer, A. Schönhals, Broadband Dielectric Spectroscopy, Springer (2003),

[6] M. Grimau, E. Laredo, M.C. Perez, A. Bello. J. Chem. Phys. 114 (2001) 64176425.

[7] L. May-Hernández, F. Hernández-Sánchez, J. L. Gómez-Ribelles, R. Sabater i Serra, J. Appl. Polym. Sci.119 (2011) 2093–2104.

[8] V. Sencadas, S. Lanceros-Mendez, R. Sabater i Serra, A. Andrio Balado, J.L. Gómez Ribelles, Eur. Phys. J. E 35 (2012) 41.

[9] L. Okrasa, P. Czech, G. Boiteux, F. Méchin, J. Ulanski, J. Non-Cryst. Solids 353, (2007) 4293–4297.

[10] A. Kanapitsas, E. Lebedev, O. Slisenko, O. Grigoryeva,P. Pissis, J. Appl. Polym. Sci 101 (2006) 1021–1035.

[11] A. Stathopoulos, P. Klonos, A. Kyritsis, P. Pissis, C. Christodoulides, J.C. Rodriguez Hernández, M. Monleón Pradas, J.L. Gómez Ribelles, Eur. Polym. J. 48 (2010) 101-111.

[12] A. Kyritsis, P. Pissis, S. Mai, C. Booth, Macromolecules 33 (2000) 4295-4606.

[13] R. Sabater i Serra, J.L. Escobar Ivirico, J.M. Meseguer Dueñas, A. Andrio Balado, J.L. Gómez Ribelles, M. Salmerón Sánchez. Eur. Phys. J. E. 22 (2007) 293-302.

[14] S. Havriliak, S. Negami, Polymer 8 (1967)161-210.

[15] P.A-M. Steeman, J. Van Turnhout, Macromolecules 27 (1994) 5421-5427.

[16] R. Richert, J. Non-Cryst Solids 305 (2002) 2456-2468.

[17] D. W. Davidson, R. H. Cole, J. Chem. Phys. 18 (1950) 1417.

[18] C.A. Angell, J. Chem. Phys. 49-8 (1988) 863-871.

[19] R. Sabater i Serra, J.L. Escobar Ivirico, J.M. Meseguer Dueñas, A. Andrio Balado, J.L. Gómez Ribelles, M. Salmerón Sanchez, J. Polym. Sci. Pt. B-Polym. Phys. 47 (2009) 183-193.

[20] R. Sabater i Serra, A. Kyritsis, J.L. Escobar Ivirico, J.L. Gómez Ribelles, P. Pissis, M. Salmerón-Sánchez, Eur. Phys. J. E (2011) 34: 37.

[21] M.T. Viciosa, N. Rousé, M. dionísio, J.L. Gómez Ribelles, Eur. Polym J. 43 (2007) 1516-1529.

[22] M.T. Viciosa, C.M. Rodríguez, M. Dionísio, J. Non-Cryst. Solids 351 (2005) 14-22.

[23] R. Sabater i Serra, M.T. Viciosa Plaza, M. Dionísio, A. Andrio Balado, J.M. Meseguer Dueñas, J.L. Gómez Ribelles, J. Non-Cryst. Solids 356 (2010) 616-620.

[24] M.T. Viciosa, A. R. Brás, J.L. Gómez Ribelles, M. Dionisio. Eur. Poly. J. 44, (2008) 155-170.

[25] M.T. Viciosa, M. Dionisio. J. Non-Cryst. Solids. 44, (2008) 155-170.

[26] H. Vogel, Phys Zeit 22 (1921) 645-646.

[27] G.S. Fulcher, J. Am. Ceram. Soc 8 (1925) 339-355.

[28] G. Tamman G, W. Hesse, Z. Anorg, Allg Chem 156 (1926), 245-257.

[29] R. Richert, A. Blumen (Eds.). Disorder Effects on Relaxational Processes, Springer, Berlin, 1994.

[30] R. Richert, A.Agapov, A.P. Sokolov, J. Chem. Phys. 134 (2011) 104508.

Table 1. Dielectric strength (Δε), shape parameters (*a*,*b*) for HN fittings and Arrhenius parameters for γ-relaxation.

γ–relaxation	NH (from -135 ºC to -85 ºC)			Arrhenius	
	Δε	*a*	*b*	*A*	*Ea* (kJmol^{-1})
CLMA 100	1.78 ± 0.10	0.26 ± 0.05	0.86 ± 0.01	1.8 ± 0.2 E-16	41 ± 1
CLMA/PEGMA 70/30	1.51 ± 0.20	0.28 ± 0.05	0.85 ± 0.01	2.4 ± 0.2 E-16	40 ± 1
CLMA/PEGMA 50/50	1.25 ± 0.10	0.29 ± 0.05	0.83 ± 0.01	3.5 ± 0.2 E-16	39 ± 1
CLMA/PEGMA 30/70	1.09 ± 0.10	0.30 ± 0.04	0.81 ± 0.01	5.1 ± 0.2 E-16	38 ± 1
PEGMA 100	0.92 ± 0.05	0.33 ± 0.05	0.80 ± 0.01	7.8 ± 0.2 E-16	38 ± 1

Table 2. VFTH parameters, dielectric glass transition temperature (τ=100 s) and activation energy at $T_{g\text{-}diel}$ for α-relaxation

α-relaxation	VTFH				
	τ_0	B	T_0	$T_{g\text{-}diel}$	$E_a(T_{g\text{-}diel})$ (kJmol^{-1})
CLMA 100	1.2 ± 0.1 E-9	1066 ± 5	230 ± 2	272 ± 2	365 ± 10
CLMA/PEGMA 70/30	4.8 ± 0.1 E-10	1340 ± 5	198 ± 2	249 ± 2	266 ± 10
CLMA/PEGMA 50/50	2.1 ± 0.1 E-10	1550 ± 5	183 ± 2	241 ± 2	222 ± 10
CLMA/PEGMA 30/70	1.1 ± 0.1 E-10	1633 ± 5	176 ± 2	235 ± 2	215 ± 10
PEGMA 100	6.2 ± 0.1 E-11	1746 ± 5	165 ± 2	227 ± 2	195 ± 10

Table 3. β parameter for Davidson-Cole function and Arrhenius parameters obtained from the relaxation times calculated from the Davidson-Cole fittings (see text) for conductivity.

conductivity (M")	Davison-Cole	Arrhenius	
	β	*A*	*Ea* (kJmol^{-1})
CLMA 100	0.86 ± 0.01	5.4 ± 0.2 E-15	81 ± 1
CLMA/PEGMA 70/30	0.85 ± 0.01	4.1 ± 0.2 E-15	71 ± 1
CLMA/PEGMA 50/50	0.83 ± 0.01	6.8 ± 0.2 E-15	68 ± 1
CLMA/PEGMA 30/70	0.81 ± 0.01	1.1 ± 0.2 E-12	50 ± 1
PEGMA 100	0.80 ± 0.01	2.8 ± 0.2 E-12	44 ± 1

Figure 1. Molecular structure of caprolactone methacrylate (CLMA), poly(ethylene gycol) methacrylate (PEGMA) and poly(CLMA-co-PEGMA).

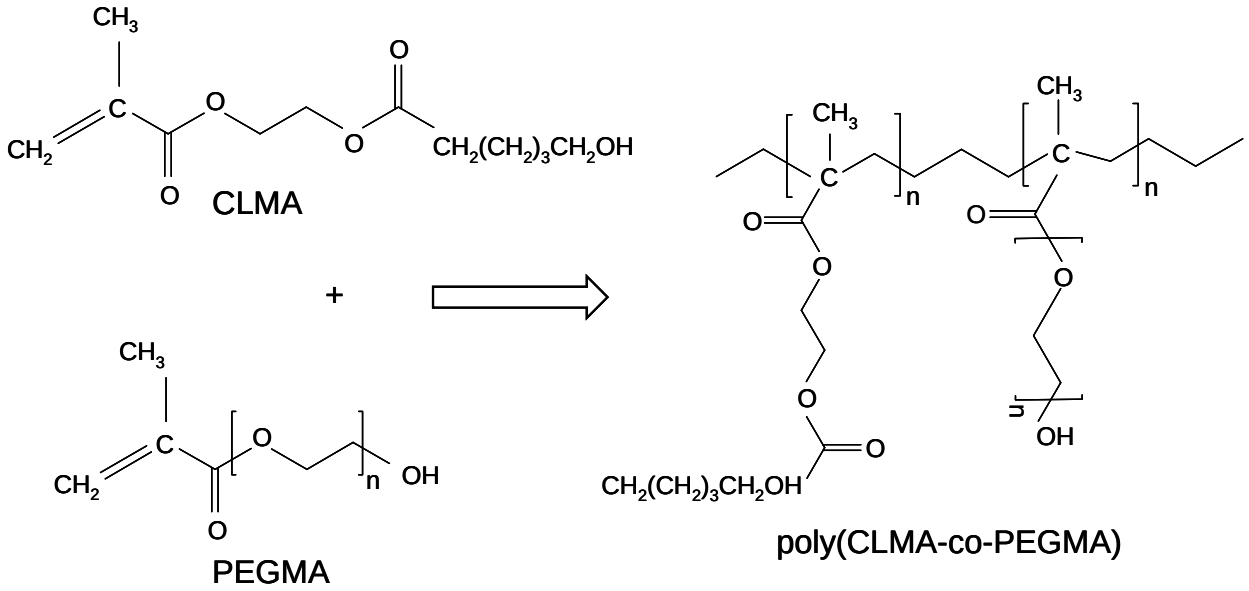

Figure 2. Frequency dependence of ε'' in polyCLMA network. Isothermal curves between -130ºC and -50ºC (a) and between 20ºC and 90ºC (b), both by steps of 10 ºC. In grey the curve at 60 ºC. The inset in plot b shows the real (open symbol) and imaginary part (full symbol) of the permittivity in the isothermal curve obtained at 60 ºC. The errors bars are smaller than the size of the symbols. The solid lines are guides to the eye.

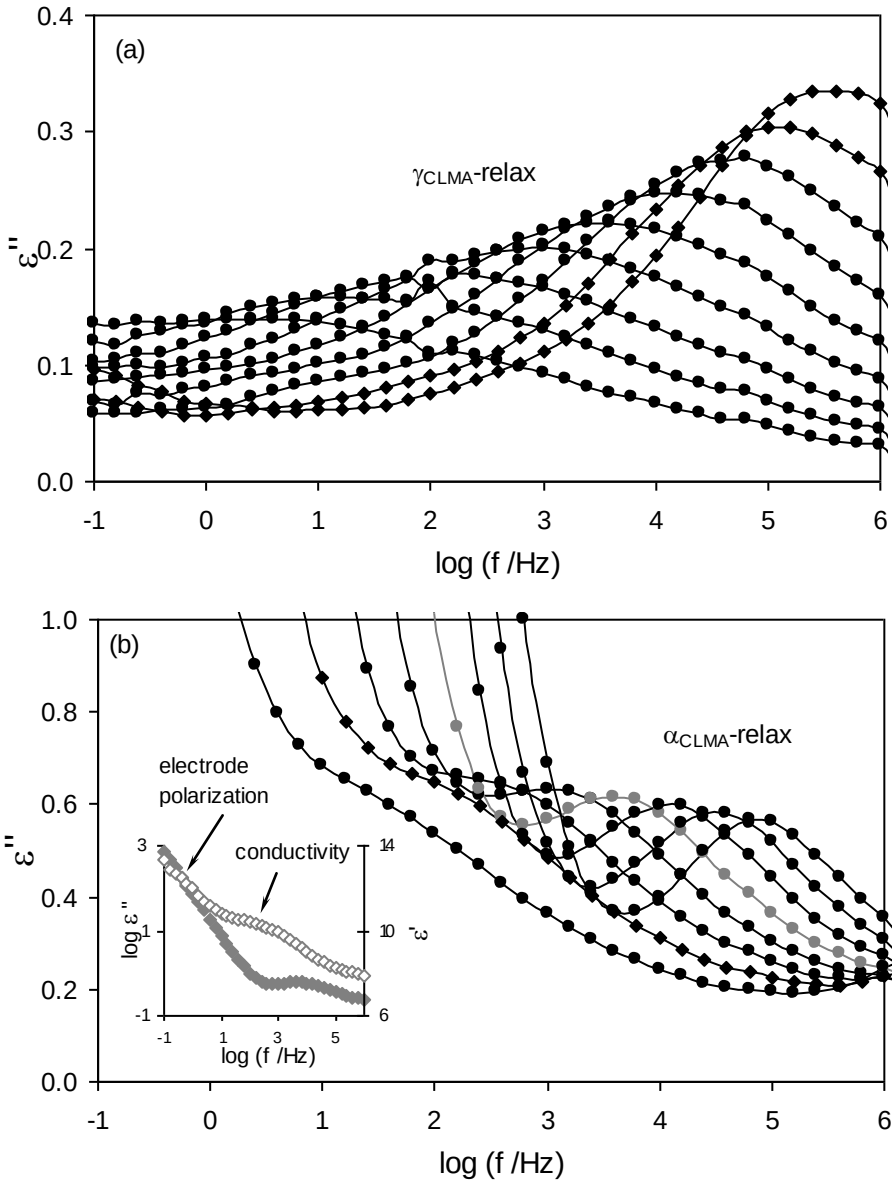

Figure 3. Temperature dependence of ε'' at 10^4 Hz. (♦) polyCLMA. (●)poly(CLMA-co-PEGMA) 70/30. (▲)poly(CLMA-co-PEGMA) 50/50. (■)poly(CLMA-co-PEGMA) 30/70. (×) polyPEGMA. The errors bars are smaller than the size of the symbols. The solid lines are guides to the eye.

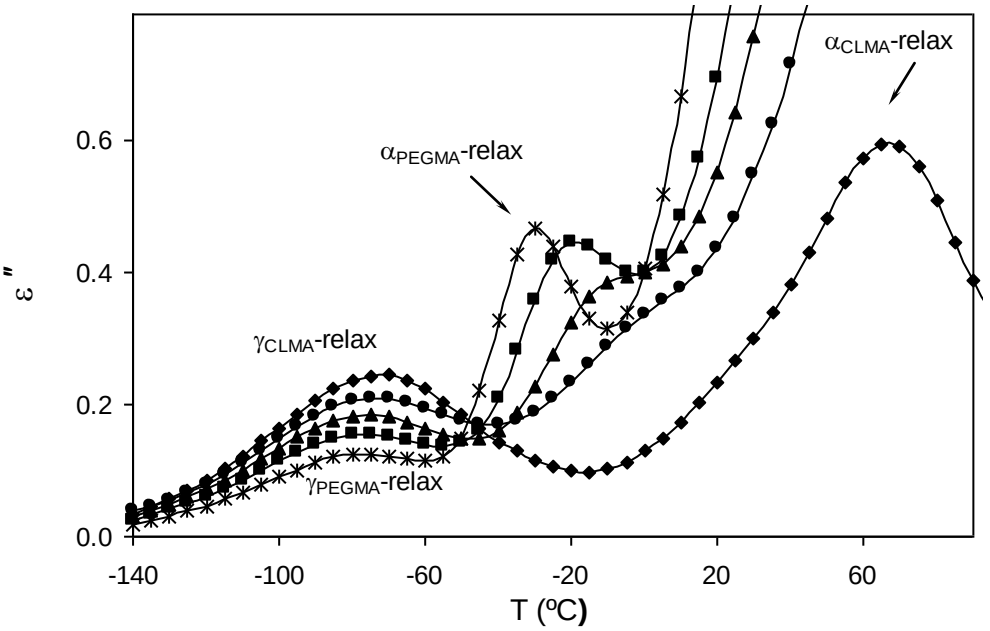

Figure 4. Frequency dependence of ε'' at 70 ºC. (♦) polyCLMA. (●) poly(CLMA-co-PEGMA) 70/30. (▲) poly(CLMA-co-PEGMA) 50/50. (■) poly(CLMA-co-PEGMA) 30/70. (×) polyPEGMA. The inset shows ε''_{der}, obtained after applying the derivative method. The errors bars are smaller than the size of the symbols. The solid lines are guides to the eye.

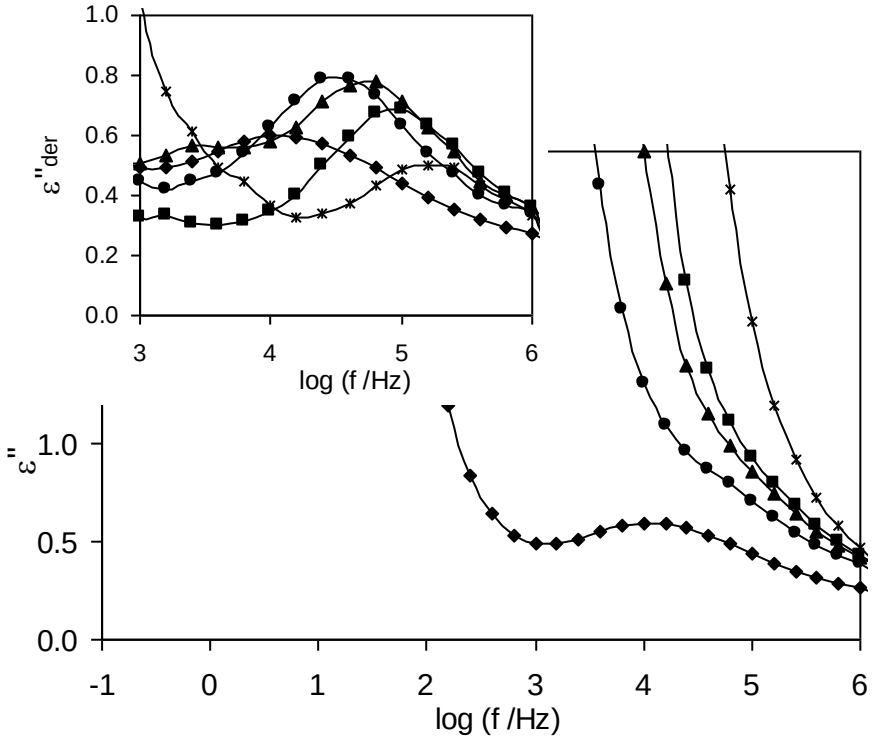

Figure 5. Dielectric loss factor ε''_{der} ,obtained applying the derivative method, from 20 ºC to 80 ºC by steps of 10ºC for poly(CLMA-co-PEGMA) 70/30 copolymer. The emphasised curve (grey) is the measurement at 50 ºC. The inset shows ε' at 50 ºC. The errors bars are smaller than the size of the symbols. The solid lines are guides to the eye.

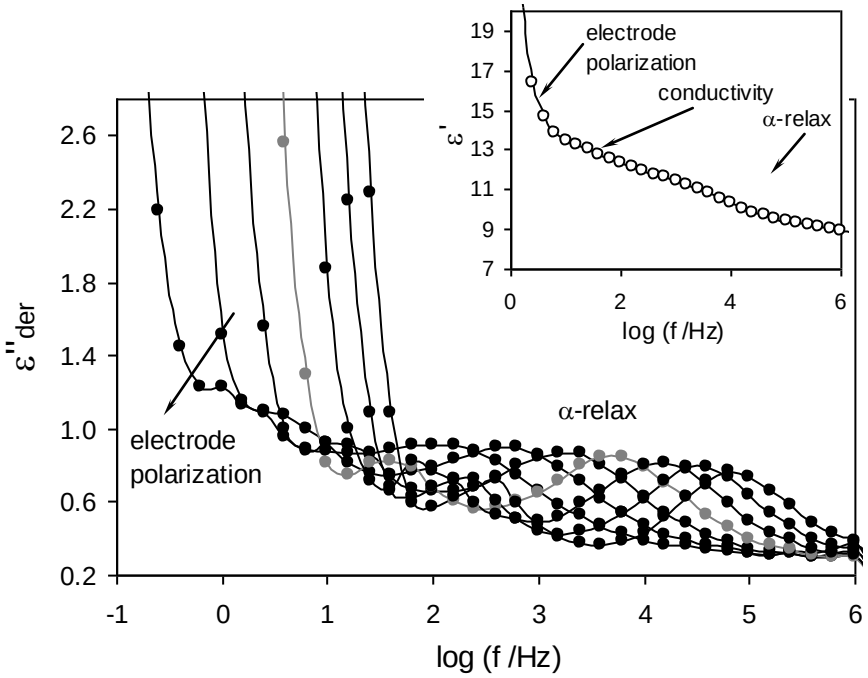

Figure 6. Frequency dependence of the real part of the conductivity (σ ') from 20 ºC to 90 ºC by steps of 10ºC in polyCLMA (a) and poly(CLMA-co-PEGMA) 50/50 (b). The inset shows the imaginary part of the conductivity (σ '') at 90ºC. The errors bars are smaller than the size of the symbols.

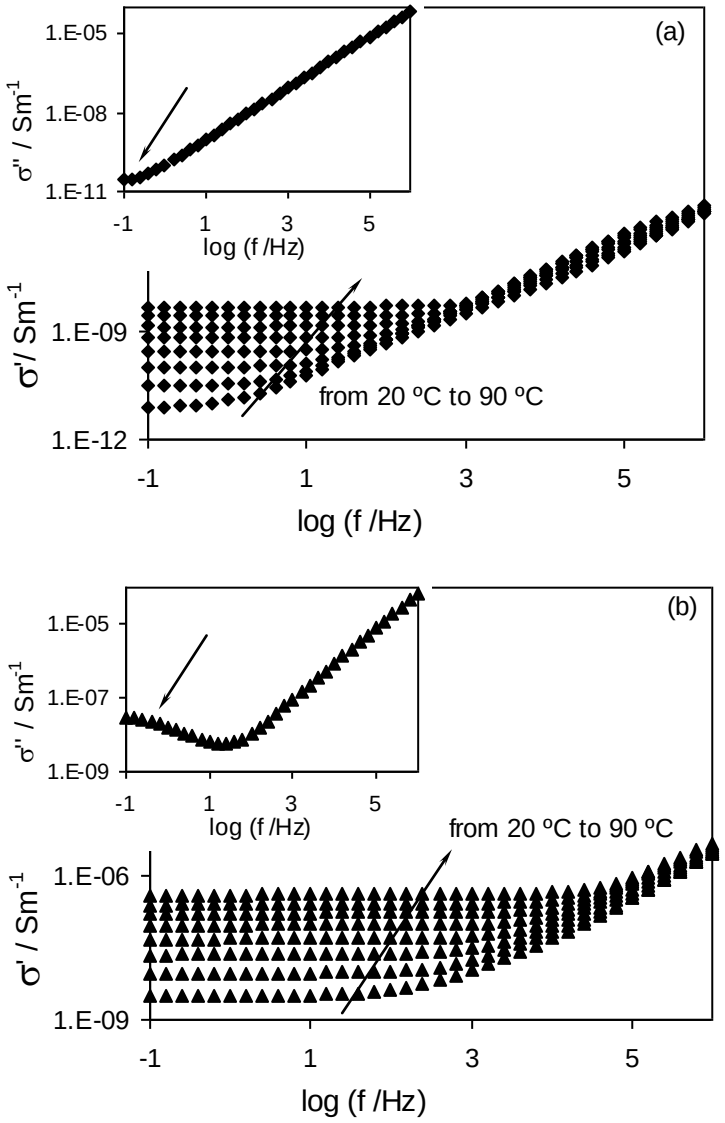

Figure 7. ε' (open symbols), ε'' (full symbol), ε'' obtained applying the derivative method (grey symbols) and the imaginary part of the electric modulus M'' (*) in function of the frequency at 80 ºC in polyCLMA (a) and poly(CLMA-co-PEGMA) 50/50 (b). The errors bars are smaller than the size of the symbols.

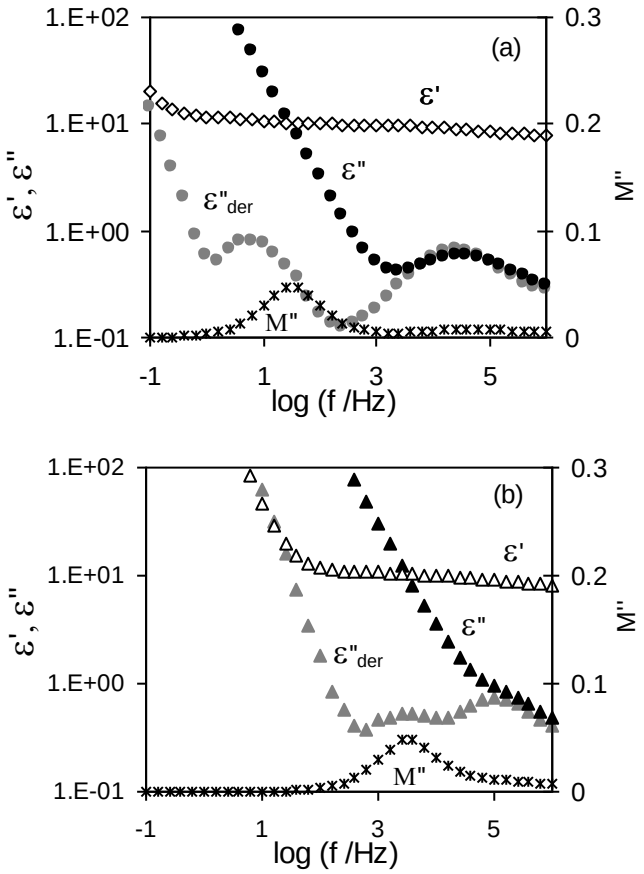

Figure 8. Temperature dependence of τ_{max} (main relaxation), τ_{HN} (γ-relaxation process), τ_{DC} (obtained applying the Davidson-Cole function in the imaginary part of the electric modulus) and the glass transition temperature obtained, from the DSC at 10 ºC/min [4]. (♦) polyCLMA. (●) poly(CLMA-co-PEGMA) 70/30. (▲) poly(CLMA-co-PEGMA) 50/50. (■) poly(CLMA-co-PEGMA) 30/70. (x) polyPEGMA. The solid lines represent the Arrhenius fit for γ-relaxation and conductivity process and the VFT fitting of the main process. Correlation coefficient $R^2 > 0.98$

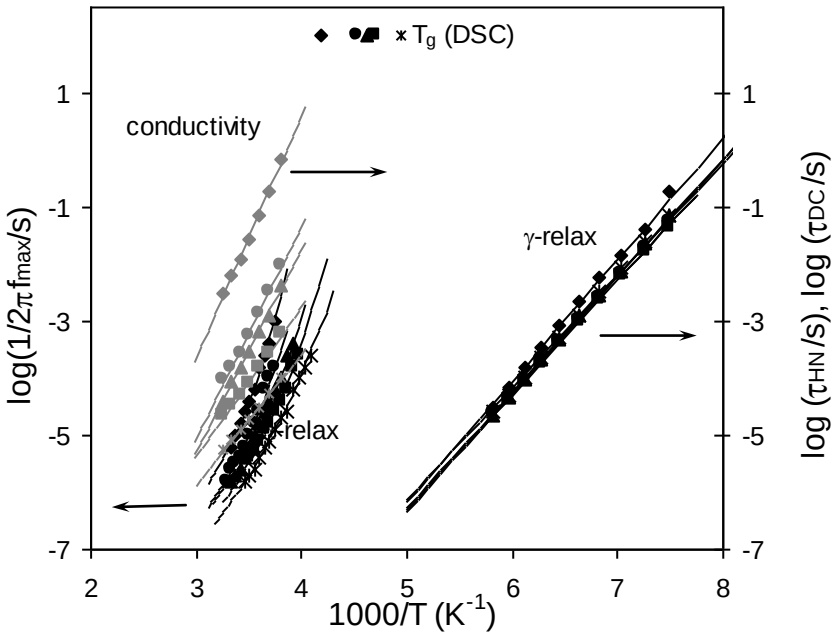

Figure 9. Relaxation times obtained from the conductivity process. τ_M from the peak in M" (full symbols), τ_c from the critical value in σ' at the end of the plateau, (gray symbols) and τ_{DC} obtained from the Davidson-Cole function (open symbols). Same symbols as those in Figure 8. The solid lines show the Davidson-Cole fitting. Correlation coefficient $R^2 > 0.98$.